Egyptian Journal of Radiology and Nuclear Medicine

RESEARCH Open Access

# Value of diffusion-weighted magnetic resonance imaging (DWI) in differentiating orbital lymphoma from idiopathic orbital inflammatory pseudotumor

Mohamed Saied Abdelgawad[1*], Walid Mohamed Ahmed Mohamed[2] and Rasha Abdelhafiz Aly[1]

## Abstract

**Background:** Diffusion-weighted MR imaging can provide physiological information complementing morphological findings from conventional MRI. It detects early tissue changes associated with changes in water content, such as changes in the permeability of cell membranes, cell swelling or cell lysis. Areas of diseased tissue are highlighted with increased signal intensity on diffusion-weighted MR imaging. A decrease in the ADC is expected with increased intracellular tissue caused by either cell swelling or increased cellular density. DWI can be performed without the need for the administration of exogenous contrast medium, so it may of use when contrast administration is contraindicated. It yields quantitative and qualitative information that reflects changes at the cellular level and indicates the integrity of cell membranes. The purpose of this study was mainly to assess the diagnostic value of DWI for the discrimination of orbital lymphoma from idiopathic orbital inflammatory pseudotumor.

**Results:** Of our 53 cases presented with proptosis or visual disturbances, 32 cases (60.4%) had found to be present with idiopathic orbital inflammatory pseudotumor and 21 cases (39.6%) had orbital lymphoma. On conventional MR imaging, ill-defined tumor margin and orbital preseptal space involvement had a significant association with orbital lymphoma, whereas intense post-contrast enhancement of lesion and radiologic evidence of sinusitis were associated with orbital inflammatory pseudotumor. The mean ADC value of orbital lymphoma was significantly lower than those of benign inflammatory pseudotumor, yielding 100% sensitivity, 99% specificity, and 90.5% accuracy for differentiating both entities.

**Conclusions:** Diffusion-weighted MR imaging (DWI) is valuable in discriminating orbital inflammatory pseudotumor from malignant orbital lymphoma that help patients to initial management.

**Keywords:** Diffusion-weighted imaging (DWI), Inflammatory pseudotumor, Lymphoma, Magnetic resonance imaging (MRI), Orbit

## Background

Idiopathic orbital inflammatory pseudotumor (IOIP) and orbital lymphoma constitute the most frequent orbital lymphoproliferative diseases [1, 2]. IOIP is an inflammatory "non-infectious" disorder of the orbit soft tissue, which usually displays indefinite morphological features [3]. Most orbital lymphomas are primary, low-grade, B-cell, non-Hodgkin lymphomas, and the frequent

*Correspondence: mselgawad@yahoo.com

[1] Radiology Department, National Liver Institute, El-Menofuia University-Shebin Elkoum, Menoufia University, Shebeen El-Kom, Egypt
Full list of author information is available at the end of the article

subtype is mucosa-associated lymphoid tissue (MALT) [4].

Lymphoma is responsive to low-dose radiotherapy with concurrent chemotherapy for only high-grade or diffuse lesions, while inflammatory pseudotumor shows a good response to corticosteroid therapy [2, 3]. Therefore, the differentiation of lymphoma and IOIP is crucial for therapeutic management. However, diffuse types of IOIPs and dacryoadenitis are misinterpreted as orbital lymphoma because of alike both clinical and imaging features [5, 6]. Even as fine-needle aspiration cytology (FNAC) is the gold differentiating method, it is likely restricted in technically challenge in the far posterior orbit lesions [7].

Previous published studies displayed MRI appearance, such as signal changes on T2 WI, presence of flow void sign and degree of post-contrast enhancement in differentiating IOIP from lymphoma [8, 9]. However, overall diagnostic value of the morphological MRI features was still restricted and may be observer-dependent during the qualitative assessment [10].

Recently, some researchers have reported the use of diffusion-weighted imaging (DWI), with the apparent diffusion coefficient (ADC) measurements to be effective in distinguishing orbital inflammatory pseudotumor from orbital lymphoma [11]. Orbital lymphoma exhibited lower mean ADC value than IOIP, yet mean ADC overlap still obtained with some controlled clinical findings. Moreover, the mean ADC value was manually got from drawing regions of interest (ROI), with possible measurement of sampling error and subjective bias [12, 13].

The focus of this study was to assess the combined value of conventional MR imaging and DWI/ADC map in discriminating orbital lymphoma from IOIP.

## Methods

### Search strategy and MR imaging

This retrospective study is based on cases with clinical suspicion of non-osseous orbital space occupying lesions. After obtaining the approval of local ethics committee, the included cases were subjected to MRI orbital study using a 1.5 Tesla MR scanner (Siemens, Magnetom Avanto, 32 channels). The head coil was used as a receiver coil. Written informed consent from patients was waived with keeping the confidentiality of medical reports.

All studied cases were subjected to complete history taking, complete ophthalmological checkup and MR scanning of the orbit. MR protocol for orbital lesions included pre-contrast series, post-contrast series and diffusion-weighted MR imaging (DWI) with the involved sequences as following: axial T1-weigthed images (TR/TE, 620/9 ms), coronal T2-weighted images (TR/TE, 4000/108 ms), axial fat-saturated T2-weighted images (TR/TE, 4000/75 ms), as well as axial, coronal and sagittal contrast-enhanced fat-saturated T1-weighted images (TR/TE, 550/9 ms). The contrast material used was Gadolinium diethylene triamine pentacetic acid (Gad-DTPA) that injected manually or as single bolus via an injector with a standard 0.1 mmol/kg dose. There were no reactions to contrast material injection in our study.

Before contrast administration, the diffusion-weighted images were obtained in the axial plane by using a single-shot echo-planar and RESOLVE sequences with the sensitivity encoding technique. DW images were generated by using the three orthogonal axis images. The used parameters were TR/TE, 4000/100 ms; section thickness, 3 mm; flip angle (FA), 90°; field of view (FOV), $200 \times 200$ mm; matrix, $384 \times 384$ and b values 0, 500 and 1000 $mm^2/s$. Diffusion-weighted images were processed to generate trace apparent diffusion coefficient (ADC) maps for the whole patients. ADC values were measured in $n \times 10^{-3}$ $mm^2/s$. Complementary non-contrast CT scanning was done when needed using MDCT 128 scanner "Aquilion 128 Toshiba Medial system, Japan."

### Image interpretation

All MR images were reviewed independently by two radiologists, with 7 and 10 years of experience, who were blinded to the clinical data as well as the histopathological findings. Concurrence between the two readers was obtained by an auxiliary reading session.

*The following data were assessed regarding the lesion*: the laterality (unilateral/bilateral), the location (intraconal, extraconal or both), the margin (well-defined or ill-defined), the signal intensity on T1-WIs, T2-WIs and post-contrast enhancement degree (mild, moderate or intense) relative to extraocular muscles (hypo-, iso-, or hyperintense) and affection of orbit preseptal space. Also, criteria indicative of sinusitis should be considered: mucosal thickening (>4 mm), fluid level or the presence of a retention cyst.

Then, quantitative assessment of DWI was performed using osirix workstation by two radiologists separately. For each case, volume of interest (VOI) was demarcated on all sections where the lesion can be seen. During image survey, T2-WI and contrast-enhanced images were used as reference to avoid intralesional necrotic areas and surrounding structures. To avoid false ADC values, the lesion periphery should be bypassed during examination. In cases with bilateral lesions, the larger lesion was assessed.

*On all lesions*, a circular region was placed over the entire lesion on "diffusion-weighted" images obtained with a b-value of 0 $s/mm^2$. This region was then copied and pasted onto the ADC maps and the corresponding ADCs were measured. ADC measurements were

repeated three times for each lesion, and the mean was calculated for further statistical analysis.

Final diagnosis was reached either by surgical findings with histopathological examination or therapeutic response or a consensus of clinical and imaging modalities.

### Statistical analysis

The data collected were tabulated and analyzed by the Statistical Package for Social Science (SPSS) version 26.0. The data were demographically organized using percentage of total, mean, median, and range for cases' ages, sex, and clinical presentations. Then, all the cases' data were described in terms of their anatomical locations as well as their conventional MRI appearances and diffusion-weighted imaging. ADC values were organized and tabulated using mean, median, range and SD ratios. Our study results were analyzed using ROC "Receiver operating characteristic" curves as well as areas under the curves to detect sensitivity and specificity of DWI and ADC imaging for the discrimination of orbital lymphoma from idiopathic orbital inflammatory pseudotumor (IOIP). The results were also tested for their significance using student "t-test."

## Results

Our study included 53 cases (27 females and 26 males) presented with proptosis or visual disturbances. Their ages ranged between 6 months and 82 years (mean age, 35.84 years and SD, 21.911).

Through a comprehensive search of our institutional medical report database over a consecutive period of 3 years (from February 2019 to January 2022), our cases were divided according to their final histopathological and clinical diagnosis into two groups: *Group A* which included 32 cases (60.4%) for benign lesions representing idiopathic orbital inflammatory pseudotumor and *Group B* which included 21 cases (39.6%) for malignant lesions representing orbital lymphoma.

*Regarding the clinical evidence,* the most common encountered symptom was proptosis in 46 out of 53 cases (86.8%), followed by orbital pain in 41 cases (77.4%). Also, 36 cases (67.9%) were presented by blurring of vision, 30 cases (56.6%) were presented by diplopia and 17 cases (32.1%) were by visual field defects. Fever, redness and hotness encountered in 15 cases (28.3%). Palpebral edema, as well as epiphora (excessive tearing), was encountered in 15 cases (28.3%), for each symptom. Three cases (5.7%) complained of unilateral sudden loss of vision, whereas unilateral gradual decrease in visual acuity was counted in 11 cases (20.8%). Ten cases (18.9%) had limited painful eye movement. Canthal swelling counting about five cases (9.4%), while the lasted encountered symptom was ptosis seen in three cases (5.7%) (Table 1).

*Radiologically*, variable MR features were found important for differentiating orbital lymphoma from IOIP. Of all the 53 cases, the characteristics of ill-defined margin (12/53, 22.6%), hyperintensity on T2 WI (9/53, 17%), and mild degree of contrast enhancement (18/53, 34%) were more frequently seen in orbital lymphoma than in IOIP. Radiologic sinusitis findings were seen significantly more often in IOIP (26/53, 49%) than in orbital lymphoma (4/53, 7.5%). Other imaging finding was included in our study, the involvement of orbit preseptal space that was detected more in lymphoma (15/53, 28.3%) than in IOIP (4/53, 7.5%).

Concerning the anatomical distribution of the lesion within the orbit, we found 23/53 cases (43.4%) with the lesion seen extraconal in location; 15 of them were IOIP and 8 were lymphoma. While 21/53 cases (39.6%) were intraconal extraocular; 17 of them were IOIP and 4 were lymphoma. The remaining nine cases (17%) were intraocular and all of them were found to be lymphoma.

*On diffusion-weighted images*, 19 out of 53 cases (35.8%) showed evident diffusion restriction appearing hypointense on ADC maps with all cases were lymphoma. While 34/53 cases (64.2%) were non-restricted with facilitated diffusion including all the 32 cases of the orbital inflammatory pseudotumors, only two cases were found to be lymphoma. The detailed qualitative MR imaging features of both entities are listed in Table 2.

*Regarding ADC values of both study groups,* the ADC values of all the 53 cases ranged from $0.13 \times 10^{-3}$ $mm^2/s$ to $2.5 \times 10^{-3}$ $mm^2/s$ with a mean ($\pm$SD) of 0.91 ($\pm 0.44$) $\times 10^{-3}$ $mm^2/s$. When, analyzing each group; the 32 cases with inflammatory pseudotumor had ADC values ranging from 0.53 to $2.5 \times 10^{-3}$ $mm^2/s$ with a mean

**Table 1** Different clinical symptoms among our cases

| Symptom | No. ($n = 53$) | %/Total |
|---|---|---|
| Orbital pain | 41 | 77.4 |
| Fever, redness and hotness | 15 | 28.3 |
| Proptosis | 46 | 86.8 |
| Palpebral edema | 15 | 23.8 |
| Canthal swelling | 5 | 9.4 |
| Limited painful eye movement | 10 | 18.9 |
| Ptosis | 3 | 5.7 |
| Epiphora (excessive tears) | 15 | 28.3 |
| Visual field defect | 17 | 32.1 |
| Blurring of vision | 36 | 67.9 |
| Diplopia | 30 | 56.6 |
| Unilateral sudden loss of vision | 3 | 5.7 |
| Unilateral gradual decrease in visual acuity | 11 | 20.7 |

**Table 2** Frequency distribution of qualitative MRI features within our cases

| Qualitative MR Features | | IOIP ($n=32$) No. (%) | Lymphoma ($n=21$) No. (%) | Total ($n=53$) No. (%) |
|---|---|---|---|---|
| Laterality | Unilateral | 24 (75) | 19 (90.5) | 43 (81.1) |
| | Bilateral | 8 (25) | 2 (9.5) | 10 (18.9) |
| Location | Extraconal | 15 (46.9) | 8 (38.1) | 23 (43.4) |
| | Intraconal/Extraocular | 17 (53.1) | 4 (19) | 21 (39.6) |
| | Intraocular | 0 (0) | 9 (42.9) | 9 (17) |
| Margin | Well-defined | 27 (84.4) | 3 (14.3) | 30 (56.6) |
| | Ill-defined | 5 (15.6) | 18 (85.7) | 23 (43.4) |
| Signal intensity on T2 WI | Hyperintense | 2 (6.3) | 9 (42.9) | 11 (20.8) |
| | Isointense | 11 (34.4) | 8 (38.1) | 19 (35.8) |
| | Hypointense | 19 (59.3) | 4 (19) | 23 (43.4) |
| DWI appearance | Restricted | 0 (0) | 19 (90.5) | 19 (35.8) |
| | Non-restricted | 32 (100) | 2 (9.5) | 34 (64.2) |
| Degree of enhancement | Moderate | 7 (21.9) | 18 (85.7) | 25 (47.2) |
| | Intense | 25 (78.1) | 3 (14.3) | 28 (52.8) |
| Orbital preseptal space involvement | Yes | 4 (12.5) | 15 (71.4) | 19 (35.8) |
| | No | 28 (87.5) | 6 (28.6) | 34 (64.2) |
| Findings suggestive of sinusitis | Yes | 26 (81.2) | 4 (19) | 30 (56.6) |
| | No | 6 (18.8) | 17 (81) | 23 (43.4) |

(±SD) of 1.15 (±0.37) × $10^{-3}$ $mm^2/s$, while the ADC values of the 21 cases with lymphoma ranged from 0.13 to 1.53 × $10^{-3}$ $mm^2/s$ with a mean (±SD) of 0.56 (±0.29) × $10^{-3}$ $mm^2/s$ (Fig. 1).

By performing the ROC analysis, with a threshold ADC value of 0.876 × $10^{-3}$ $mm^2/s$, ADC showed 100% sensitivity, 99% specificity, and 90.5% accuracy for differentiating orbital lymphoma from IOIP. Unpaired independent

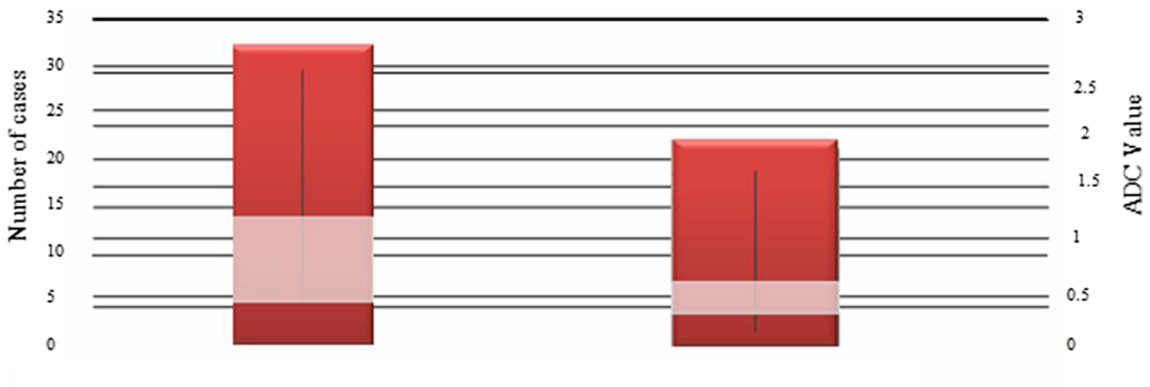


| | IOIP | Lymphoma |
|---|---|---|
| Number | 32 | 21 |
| SD | 0.37 | 0.29 |
| Maximum | 2.5 | 1.53 |
| Minimum | 0.53 | 0.13 |
| Mean | 1.15 | 0.56 |

**Fig. 1** Descriptive analysis of mean, SD and range of ADC values in both studied entities

2-sample Student "t-test" for means of the ADC values was done to detect significance of the results of the ROC curve for both study groups expressing that the p value < 0.0001 for all the test results *(Highly significant).*

## Discussion

Differentiation of orbital inflammatory pseudotumor and orbital lymphoma has a treatment planning benefit. The clinical differentiation between these two entities is limited. Therefore, there is a need for an effective and non-invasive method to differentiate them. MRI plays an important role in evaluating the orbital lesions and provides supplementing information beyond clinical examination [10].

Orbital lymphoma is generally present with a progressive course of low-grade proptosis and minimal pain, whereas IOIP generally presents more acutely, with symptoms of proptosis, ocular motility disturbance, pain, erythema, and chemosis. Nonetheless, these features can be common to both entities with a variable onset and both commonly present as a mass on CT and MR imaging, further complicating the distinction between these diseases [14].

Prior studies [15, 16] indicated that some specific MR imaging features such as lesion shape, the involvement of orbit preseptal space and imaging findings suggestive of sinusitis might be potentially useful for differentiating inflammatory pseudotumor from lymphoma. However, the qualitative assessment of MRI features is a subjective process with limited interreader reproducibility, hence indicating a need for more objective methods to improve the diagnostic accuracy and confidence.

Concerning the conventional MR imaging in our literature, most inflammatory pseudotumor patients were having T1 hypointense and T2 isointense signals, whereas lymphomas showed mildly hyperintense signal on T2 compared to extraocular muscles but can show variability.

We found orbit preseptal space affection was commonly observed in orbital lymphomas than IOIPs. *Nasser* et al. [17] reported that nearly half of orbit lymphoma lesions were located in conjunctiva, and *Gerbino* et al. [18] detected that eyelid was involved in 35% of orbital lymphomas. We also found that imaging findings indicative of sinusitis were more commonly seen in IOIP than orbital lymphoma. *Haradome* et al. [9] *and Xu* et al. [10] have shown an extension of inflammatory changes to the paranasal mucosa in orbital inflammatory disorders.

In our study, intense post-contrast enhancement was observed more frequently in cases with orbital inflammatory pseudotumor. *Haradome* et al. [9] reported that the degree of inflammatory pseudotumor enhancement was significantly higher than that of lymphoma, suggesting its hypervascular nature.

Previous descriptive analyses, comparing IOIP and lymphoma on conventional MR imaging, did not show differences specific enough for differentiating these diseases. Because the clinical findings and morphological MRI findings in both entities often have considerable overlap, it can be difficult to make a definitive diagnosis without a pathologic specimen. Therefore, it would be clinically useful to have a non-invasive method to help distinguish these processes, yielding the value of diffusion-weighted MR imaging in differentiating both lesions [19].

In agreement with previous studies, [20–23] we found that the mean ADC of orbital lymphoma ($0.56 \times 10^{-3}$ mm$^2$/s) was significantly lower than that of IOIP ($1.15 \times 10^{-3}$ mm$^2$/s). It is suspected that the uniformly and atypical lymphocyte infiltrations in orbital lymphoma lead to higher cellularity and less extracellular space with subsequent low ADC value [24]. However, two cases with lymphoma show high ADC value as some previous studies [25 and 26] mentioned that the small necrotic foci in the malignant tumor, which are not identifiable at MRI, are considered the major reason for that finding. Regarding the benign IOIP, interstitial edematous changes in this lesion give rise to high ADC value promoting a significant ADC value difference [27].

Our studies orbital lesions were identified at an optimal threshold ADC value of $0.876 \times 10^{-3}$ mm$^2$/s, that showed about 100% sensitivity, as well as 99% specificity for differentiating orbital inflammatory pseudotumor (Figs. 2, 3, 4, 5, 6) from orbital lymphoma (Figs. 7, 8, 9, 10, 11), indicating the significant role of ADC values in discriminating both entities. The previous results were comparable to that of *Xu* et al. [10]. *The aforementioned study* conducted a similar randomized trial on DWI/ADC imaging role in differentiating orbital lymphoma from IOIP with nearly similar results having 90.9% sensitivity and specificity 100% using ADC cutoff value of $0.886 \times 10^{-3}$ mm$^2$/s in their study.

## Conclusions

In conclusion, diffusion-weighted MR imaging (DWI) is valuable in discriminating orbital inflammatory pseudotumor from malignant orbital lymphoma that may help triage patients to either early intervention or initial conservative treatments. So, we recommend introduction of DWI as routine sequence in all MRI examinations of the orbit to minimize the need for invasive diagnostic method.

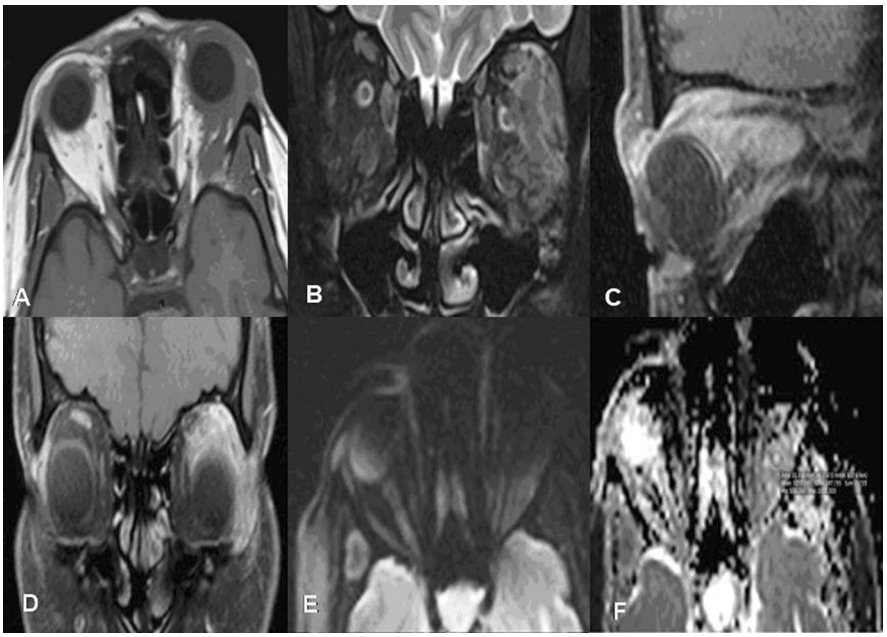


**Fig. 2** A 56-year-old male with acute sinusitis presented with left-sided orbital pain and blurring of vision. Axial T1-weighted image **A** shows hypointense signal involving the sclera of left eye, the related intra- and extraconal fat planes and the lateral rectus muscle. Coronal T2-weighted image **B** shows an extraconal mass involving the left lateral rectus muscle, the lacrimal gland with intraconal extension. Post-contrast T1 fat-saturated images **C**,**D** show homogeneous enhancement of the extraconal mass and its intraconal component. No diffusion-weighted restriction seen on DWI ($b_{500}$) (**E**) and ADC **(F)**. The ADC value for the lesion is $1.27 \times 10^{-3}$ $mm^2$/ sec. FNAC of the mass proved to be left-sided orbital inflammatory pseudotumor

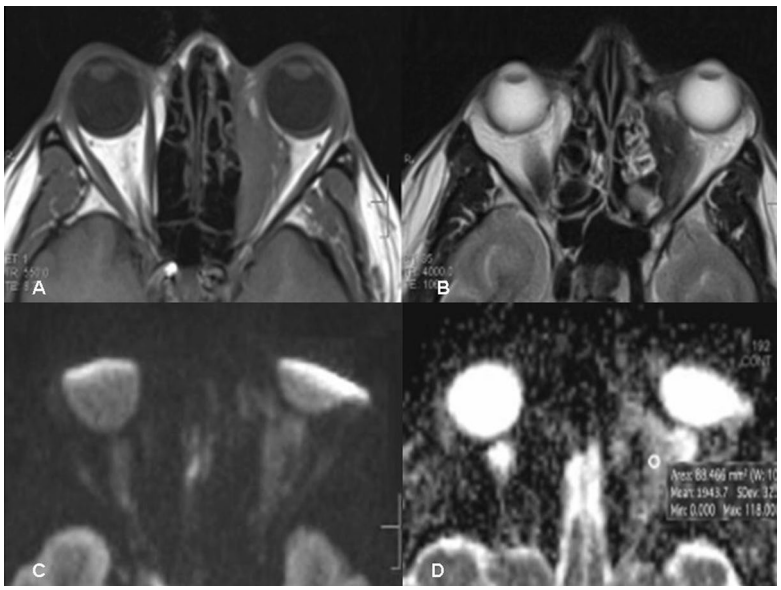


**Fig. 3** A 13-year-old male with acute pan-sinusitis; presented with right-sided dull aching orbital pain, mild proptosis and limited orbital gaze. Axial T1 image (**A**) shows diffusely enlarged right superior and medial recti with mild haziness of the right intraconal retro bulbar fat. Axial T2 image (**B**) shows diffuse enlargement of the right superior and medial recti muscles with mild hyperintense signal. No diffusion weighted restriction seen on DWI ($b_{500}$) image (**C**) and ADC (**D**). The ADC value is $1.34 \times 10^{-3}$ $mm^2$/sec. Right-sided orbital inflammatory pseudotumor, Myositic type. Therapeutic trial with corticosteroids was done and the patient relieved after 5 weeks

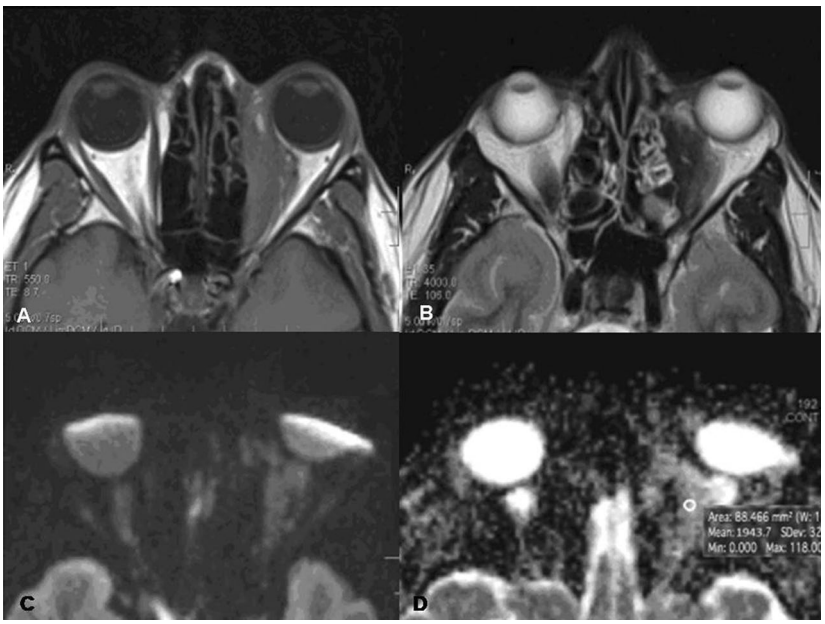


**Fig. 4** A 35-year-old female patient with acute rhino-sinusitis presented with left-sided orbital pain, mild proptosis and limited orbital movement. Axial T1- and T2-weighted images of the left orbit **A**, **B** show a primarily extraconal mass involving the left medial rectus muscle with intraconal extension. No diffusion-weighted restriction seen on DWI ($b_{500}$) image (**C**) and ADC (**D**). The ADC value for the mass is $1.09 \times 10^{-3}$ $mm^2/s$. Histopathologically proved left-sided orbital inflammatory pseudotumor by FNAC

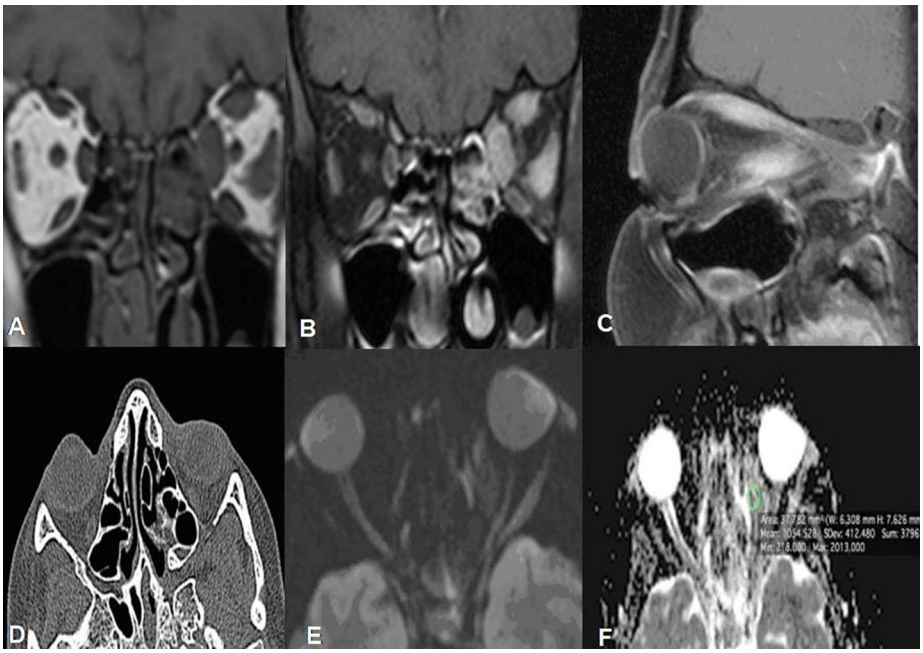


**Fig. 5** A 23-year-old male patient with acute rhino-sinusitis presented with left-sided orbital pain, mild proptosis and limited orbital gaze. Coronal T1 **A** shows diffusely enlarged left superior, medial and lateral recti with mild stranding of the left retrobulbar fat. Coronal and sagittal T1 fat-sat post-contrast images **B**, **C** show homogeneous enhancement of these left orbital muscles. Axial non-contrast CT image bone window **D** reveals ethmoidal and sphenoidal mild sinusitis. No diffusion-weighted restriction seen on DWI ($b_{500}$) **E** and ADC **F**. The ADC value is $1.05 \times 10^{-3}$ $mm^2$/sec. Left-sided orbital inflammatory pseudotumor, Myositic type; responded well 2 weeks after therapeutic trial with corticosteroids

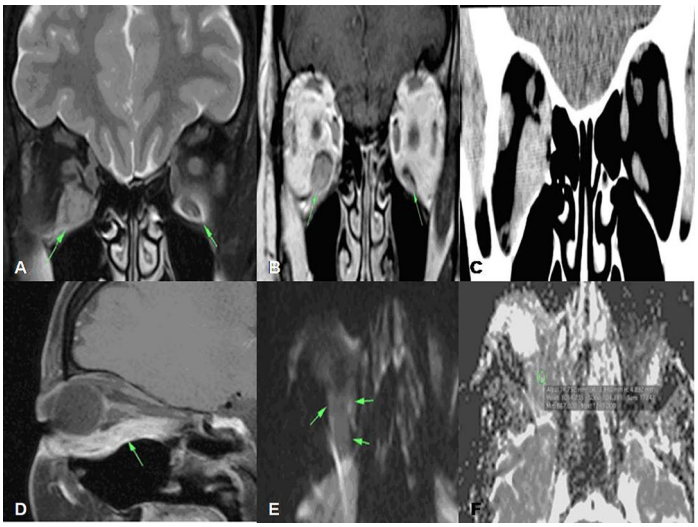


**Fig. 6** A 34-year-old male patient with acute onset of right-sided dull aching orbital pain and limited orbital movement Coronal T2WI and T1WI images **A**, **B** show enlarged right inferior and lateral recti muscles displaying T1 and T2 isointense signal with minor similar changes involving the left inferior rectus muscle. Complementary non-enhanced CT coronal image **C** shows bulky right inferior muscle and to lesser extent right lateral rectus muscle. Contrast-enhanced sagittal T1 fat-saturated image **D** shows marked contrast enhancement of inferior rectus muscle bulk. No diffusion-weighted restriction seen on DWI ($b_{500}$) (**E**) and ADC (**F**). The ADC value is $1.1 \times 10^{-3}$ $mm^2$/sec. Right-sided orbital inflammatory pseudotumor, Myositic type; responded well 2 weeks after therapeutic trial with corticosteroids

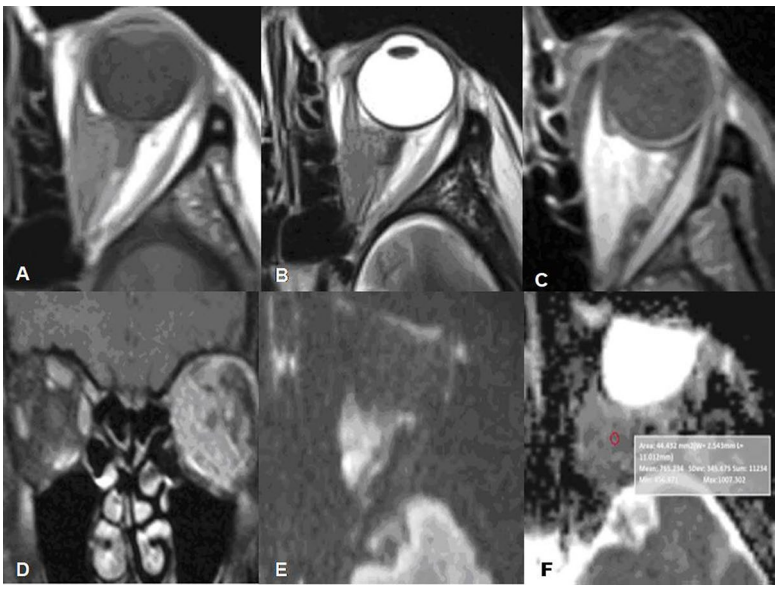


**Fig. 7** A 56-year-old female patient with long history of left-sided dull aching orbital pain, chronic visual loss of left eye and limited left orbital movement. Axial T1 **A** shows T1 hypointense infiltrative retrobulbar mass involving the left medial rectus muscle, as well as the related extraconal and intraconal fat planes and encasing the optic nerve. Axial T2 image **B** shows ill-defined T2 hypointensity of the lesion. Axial and coronal T1 post-contrast images **(C and D)** reveal homogeneous enhancement of the mass lesion. Evident diffusion restriction on DWI ($b_{1000}$)/ADC (**E**, **F**). The ADC value is $0.76 \times 10^{-3}$ $mm^2$/sec (F). Pathologically proved left-sided retrobulbar lymphoma (NHL) encasing the left optic nerve

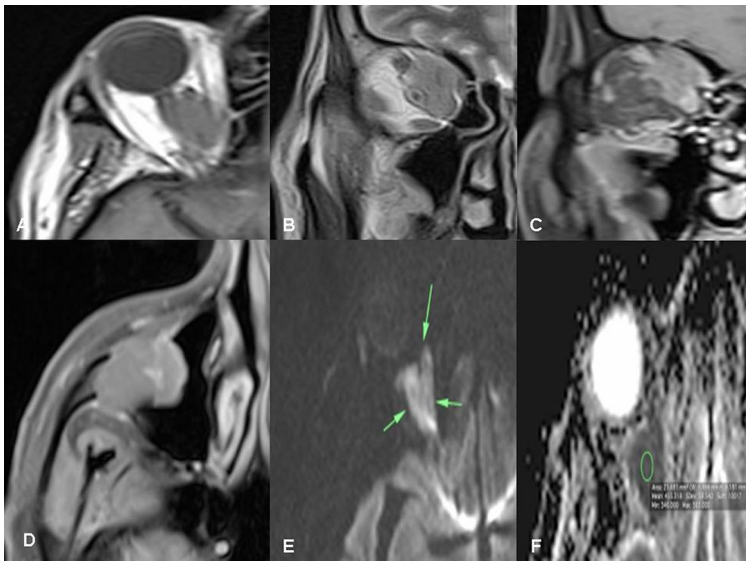


**Fig. 8** A 59-year-old female with right-sided dull aching orbital pain and limited right orbital movement. Axial T1 image **A** shows T1 hypointense infiltrative right retrobulbar intraconal mass involving the right medial rectus muscle, the related intraconal fat planes and inseparable from the optic nerve. Coronal T2 image **B** shows isointense signal of the lesion. Coronal T1 post-contrast image **C** reveals homogeneous enhancement of the retrobulbar lesion with possible invasion of the orbital roof. Axial T1 post-contrast image **D** shows similar infiltrative submucosal mass seen in the left maxillary sinus. Evident diffusion restriction on DWI ($b_{1000}$)/ADC (**E**, **F**). The ADC value of $0.46 \times 10^{-3}mm^2$/sec. **E** Pathologically proved right-sided retrobulbar lymphoma (NHL) partially encasing the left optic nerve

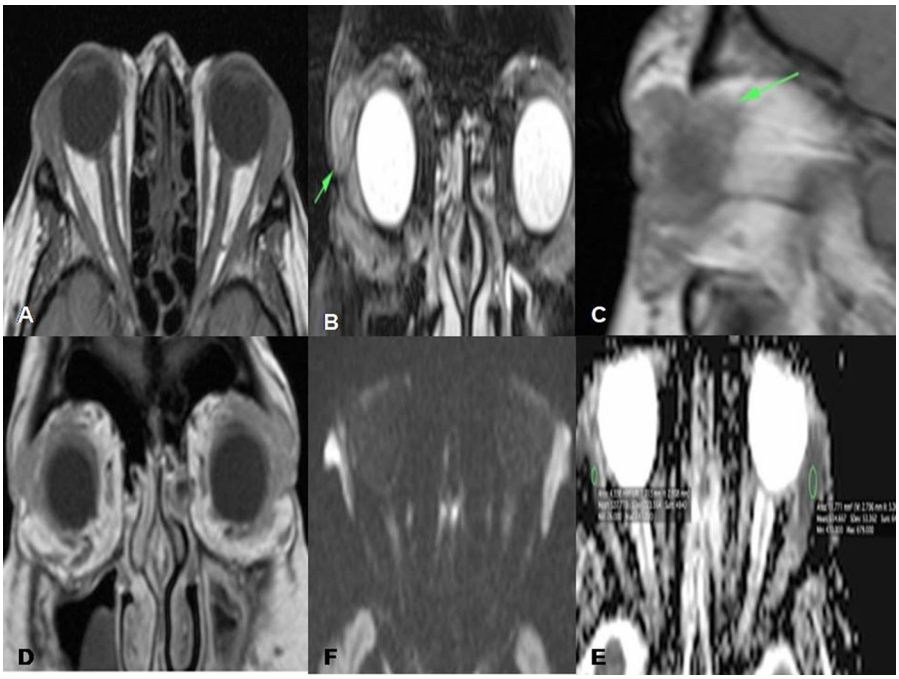


**Fig. 9** A 57-year-old male bilateral dull aching orbital pain, epiphora and cervical lymphadenopathy. Axial T1 image **A** shows T1 hypointense infiltrative masses involving both lacrimal glands. Coronal T2 image **B** revealed hyperintense signal of the lesions. Sagittal T1 post-contrast **C** reveals homogeneous mild enhancement of the previously mentioned both lacrimal gland masses. (arrow) Coronal T1 post-contrast image **D** shows mild enhancement of the lacrimal gland lesions. Evident diffusion restriction on DWI ($b_{1000}$)/ADC (**E**, **F**). The ADC value for the left mass is $0.53 \times 10^{-3}mm^2$/ sec (**F**). Bilateral lacrimal gland lymphomas, proved by histopathology and hematological study

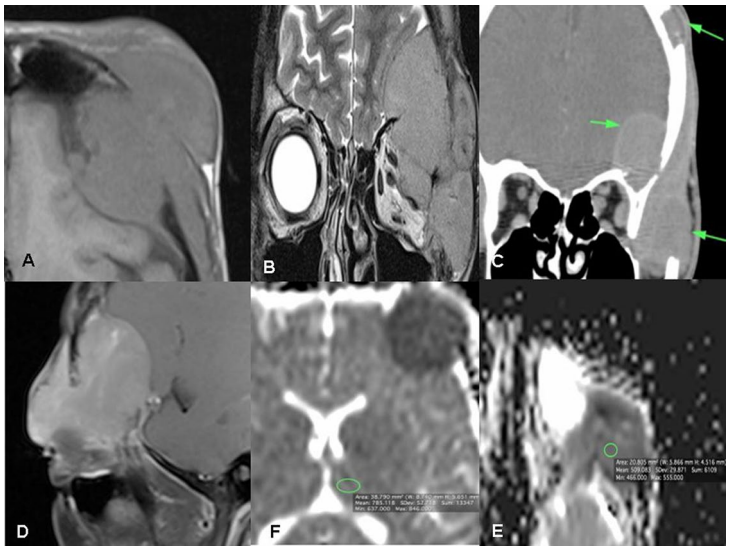


**Fig. 10** A 26-year-old female rapidly growing swelling in the lateral aspect of the left orbit, associated with proptosis, headache and dull aching left orbital pain and cervical lymphadenopathy. Axial T1 image **A** shows hypointense infiltrative mass involving the left lacrimal gland, the left extraconal fat, the lateral bony wall, the left side of skull base, as well as the roof of the left orbit, and has a related left frontal epidural component. Coronal T2 image **B** shows slightly hyperintense mass displacing the extraconal muscles and the left optic nerve infero-medially. Non-contrast complementary CT study soft tissue window C reveals bone destruction of the left lateral orbital wall, left orbital roof, and lesser wing of sphenoid bone (green arrows). Sagittal T1 post-contrast image **D** shows mild enhancement of the left orbital mass. Evident diffusion restriction on DWI ($b_{1000}$)/ADC (**E**, **F**). The ADC value of $0.52 \times 10^{-3}mm^2/sec$. Pathologically proved left orbital extraconal infiltrative lymphoma

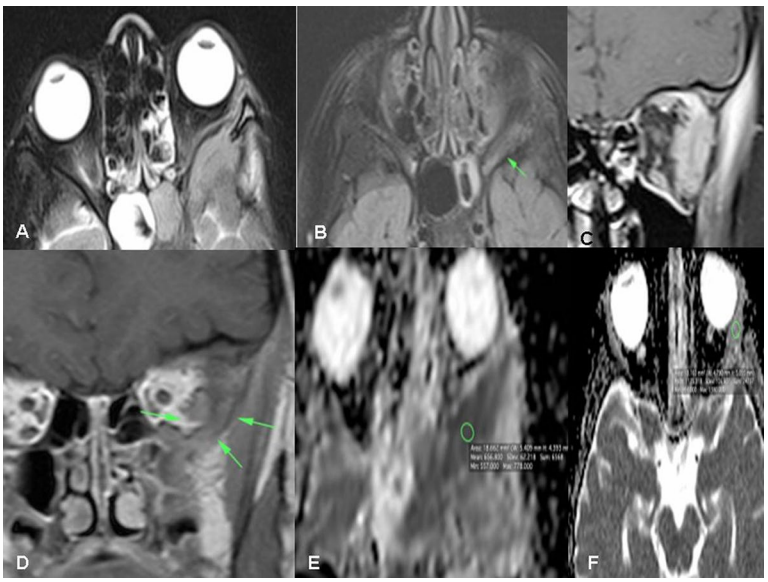


**Fig. 11** A 14-year-old male patient with history of rapid left-sided proptosis, swelling in the lateral aspect of the left orbit and dull aching left orbital pain. Initial orbital MRI with contrast was done. Axial T2-weighted image **A** shows hypointense infiltrative mass involving the left extraconal fat, the lateral bony wall, the left sphenoid bone and sinus, with left temporal epidural component. Axial FLAIR follow-up image **B** shows isointense signal with reduction in mass size and loss of its epidural component as compared to the initial MRI study. Coronal post-contrast T1-weighted image **C** shows an enhancing left lateral extraconal mass in the left orbit Follow-up coronal post- contrast T1-image **D** shows marked reduction in the mass size and enhancement. Evident diffusion restriction on DWI ($b_{1000}$)/ADC (**E**, **F**). The ADC value of $1.12 \times 10^{-3}mm^2/s$. Pathologically proved left orbital extraconal infiltrative lymphoma

**Abbreviations**
ADC: Apparent diffusion coefficient; DWI: Diffusion-weighted imaging; FNAC: Fine-needle aspiration cystology; IOIP: Idiopathic orbital inflammatory pseudotumor; Gad-DTPA: Gadolinium diethylene triamine pentacetic acid; MALT: Mucosa-associated lymphoid tissue; MDCT: Multidetector computed tomography; MRI: Magnetic resonance imaging; RESOLVE: Readout segmentation of long variable echo trains; ROC: Receiver operating characteristic curve; ROI: Region of interest; SD: Standard deviation; SPSS: Statistical Package for Social Science; TE: Echo time; TR: Repetition time; VOI: Volume of interest; WI: Weighted image.

**Acknowledgements**
Not Applicable.

**Author contributions**
MSA carried out cases on workstation and selection of research cases, prepared the figures for cases demonstration, and contributed to writing and review of the research. WMAM assesses in cases selection and follow-up. RAA contributed to writing the research, sharing in selection of the cases; sharing in figures preparation of cases. "All authors read and approved the final manuscript."

**Funding**
This study had no funding from any resource.

**Availability of data and materials**
The datasets used and/or analyzed during the current study are available from the corresponding author on reasonable request.

## Declarations

**Ethics approval and consent to participate**
All procedures followed were in accordance with the ethical standards of the responsible committee on human experimentation Institutional Review Board (IRB) of National Liver Institute Menoufia University and with the Helsinki Declaration of 1964 and later versions. Committee's reference number is unavailable (NOT applicable). No consent was obtained from the patients since it was a retrospective study.

**Consent for publication**
All patients included in this research gave written informed consent to publish the data contained within this study.

**Competing interests**
The authors declare that they have no competing interests.

**Author details**
[1]Radiology Department, National Liver Institute, El-Menofuia University-Shebin Elkoum, Menoufia University, Shebeen El-Kom, Egypt. [2]Radiology Department, Medical Research Institute, Alexandria University, Alexandria, Egypt.

Received: 10 August 2022 Accepted: 29 October 2022
Published online: 09 November 2022

**References**

1. Li EY, Yuen HK, Cheuk W (2015) Lymphoproliferative disease of the orbit. Asia Pac J Ophthalmol (Phila) 4(2):106–111
2. Watkins LM, Carter KD, Nerad JA (2011) Ocular adnexal lymphoma of the extraocular muscles: case series from the University of Iowa and review of the literature. Ophthalmic Plast Reconstr Surg 27(6):471–476
3. Ding ZX, Lip G, Chong V (2011) Idiopathic orbital pseudotumour. Clin Radiol 66(9):886–892
4. Go H, Kim JE, Kim YA (2012) Ocular adnexal IgG4-related disease: comparative analysis with mucosa-associated lymphoid tissue lymphoma and other chronic inflammatory conditions. Histopathology 60:296–312
5. Briscoe D, Safieh C, Ton Y, Shapiro H, Assia E, Kidron D (2018) Characteristics of orbital lymphoma: a clinicopathological study of 26 cases. Int Ophthalmol 38:271–277
6. Gokharman D, Aydin S (2018) Magnetic resonance imaging in orbital pathologies: a pictorial review. J Belg Soc Radiol 102(1):1–8
7. Yan J, Wu Z, Li Y (2004) The differentiation of idiopathic inflammatory pseudotumor from lymphoid tumors of orbit: analysis of 319 cases. Orbit 23(4):245–254
8. Ren J, Yuan Y, Wu Y, Tao X (2018) Differentiation of orbital lymphoma and idiopathic orbital inflammatory pseudotumor: combined diagnostic value of conventional MRI and histogram analysis of ADC maps. BMC Med Imaging 18:6
9. Haradome K, Haradome H, Usui Y, Ueda S, Kwee TC, Saito K (2014) Orbital lymphoproliferative disorders (OLPDs): value of MR imaging for differentiating orbital lymphoma from benign OPLDs. AJNR Am J Neuroradiol 35(10):1976–1982
10. Xu XQ, Hu H, Liu H, Wu JF, Cao P, Shi HB (2017) Benign and malignant orbital lymphoproliferative disorders: differentiating using multiparametric MRI at 3.0T. J Magn Reson Imaging 45(1):167–176
11. Politi LS, Forghani R, Godi C, Resti AG, Ponzoni M, Bianchi S (2010) Ocular adnexal lymphoma: diffusion-weighted MR imaging for differential diagnosis and therapeutic monitoring. Radiology 256(2):565–574
12. Jaju A, Rychlik K, Ryan ME (2020) MRI of pediatric orbital masses: role of quantitative diffusion-weighted imaging in differentiating benign from malignant lesions. Clin Neuroradiol 30:615–624
13. Soliman AF, Aggag MF, Abdelgawwad AE, Aly WE, Youssef A (2020) Role of diffusion weighted MRI in evaluation of orbital lesions. Al-Azhar Int Med J. https://doi.org/10.21608/aimj.22010.1053
14. Patnana M, Sevrukov AB, Elsayes KM, Viswanathan C, Lubner M, Menias CO (2012) Inflammatory pseudotumor: the great mimicker. AJR 198(3):W217–W227
15. Xu XQ, Hu H, Su GY, Zhang L, Liu H, Shi HB, Hong XN (2016) Diffusion weighted imaging for differentiating benign from malignant orbital tumors: diagnostic performance of the apparent diffusion coefficient based on region of interest selection method. Korean J Radiol 17(5):650–656
16. Kim MK, Jang SY, Jang JW (2013) Clinical characteristics of pediatric orbital pseudotumors. J Korean Ophthalmol Soc 54(6):850–856
17. Nasser Q, Pfeiffer M, Romaguera J, Fowler N, Debnam M, Samaniego F, El-Sawy T, McLaughlin P, Bakhoum M, Esmaeli B (2013) Clinical value of magnetic resonance imaging and other baseline testing for conjunctival mucosa-associated lymphoid tissue lymphoma. Leuk Lymphoma 55:1013–1017
18. Gerbino G, Boffano P, Benech R, Baietto F, Gallesio C, Arcuri F (2014) Orbital lymphomas: clinical and radiological features. J Craniomaxillofac Surg 42(5):508–512
19. Kapur R, Sepahdari AR, Mafee MF (2009) MR imaging of orbital inflammatory syndrome, orbital cellulitis, and orbital lymphoid lesions: the role of diffusion-weighted imaging. AJNR Am J Neuroradiol 30:64–70
20. Öztürk M, Sayıt AT, Çelenk C, Yeter V (2022) Diagnostic value of diffusion-weighted MRI and conventional MRI in the differentiation of benign and malignant orbital lesions. Cukurova Med J 47(1):34–43
21. Fatima Z, Ichikawa T, Ishigame K, Motosugi U, Waqar AB, Hori M (2014) Orbital masses: the usefulness of diffusion-weighted imaging in lesion categorization. Clin Neuroradiol 24(2):129–134
22. Sepahdari AR, Politi LS, Aakalu VK, Kim HJ, Abdel Razek AA (2014) DWI of orbital masses: multi-institutional data support a 2-ADC threshold model to categorize lesions as benign, malignant, or indeterminate. AJNR 35:170–175
23. Ro SR, Asbach P, Siebert E, Bertelmann E, Hamm B, Erb-Eigner K (2016) Characterization of orbital masses by multiparametric MRI. In Eur J Radiol 85(2):324–336
24. WuX PH, Dastidar P (2013) ADC measurements in diffuse large B-cell lymphoma and follicular lymphoma: a DWI and cellularity study. Eur J Radiol 82:e158–e164
25. Sepahdari AR, Aakalu VK, Setabutr P, Shiehmorteza M, Naheedy JH, Mafee MF (2010) Indeterminate orbital masses: restricted diffusion at MR imaging with echo-planar diffusion-weighted imaging predicts malignancy. Radiology 256:554–564
26. Wang J, Takashima S, Takayama F, Kawakami S, Saito A, Matsushita T (2001) Head and neck lesions: characterization with diffusion-weighted echo-planar MR imaging. Radiology 220:621–630

27. Mundhada P, Rawat S, Acharya U, Raje D (2021) Role of quantitative diffusion-weighted imaging in differentiating benign and malignant orbital masses. Indian J Radiol Imaging 31:102–108

## Publisher's Note